Proceedings of the 11th World Congress on Mechanical, Chemical, and Material Engineering (MCM'25)

Paris, France - August, 2025 Paper No. HTFF 113 DOI: 10.11159/htff25.113

# Improving Interferometric Heat Transfer Measurements in Nanofluids with Centrifugation and SDBS Stabilization

### S. Sahamifar <sup>1</sup>, D. Naylor, J. Friedman

Department of Mechanical, Industrial, and Mechatronics Engineering, Toronto Metropolitan University 350 Victoria St., Toronto, Canada, M5B 2K3

1ssahamifar@torontomu.ca

**Abstract** - Ensuring the stability of the working nanofluid throughout heat transfer experiments is essential for obtaining reliable results. This study uses a newly developed interferometric method to visualize and quantify nanofluid uniformity and stability. It is shown that nonuniformities in the nanofluid can cause significant errors in interferometric heat transfer measurements. To mitigate such errors, several techniques are employed to improve nanofluid stability. The nanofluid, initially prepared by sonication, underwent sedimentation and centrifugation at 1500 g for 90 minutes. Additionally, sodium dodecylbenzene sulfonate (SDBS) was added to the centrifuged sample to assess the impact of surfactants. Results indicate that both centrifugation and SDBS enhance nanofluid stability. A 0.23 wt.% Al<sub>2</sub>O<sub>3</sub>-water nanofluid with 0.23 wt.% SDBS was produced, remaining stable for 1.5 hours, a sufficient duration for heat transfer measurements.

Keywords: Al<sub>2</sub>O<sub>3</sub> nanofluid, SDBS, Stability improvement, Centrifugation, Interferometry, Heat transfer errors

#### 1. Introduction

Nanofluids have attracted significant attention over the past two decades due to their potential to enhance thermophysical properties and improve heat transfer [1]. This growing interest has led researchers to adopt interferometric techniques to investigate nanofluid heat transfer, as these methods provide deeper insights into the underlying mechanisms [2-4]. However, the accuracy of interferometric methods can be significantly affected by nonuniformity in nanofluids, which introduces substantial errors in heat transfer measurements [5, 6]. This paper investigates methods for producing a uniform and stable nanofluid through a new interferometric technique to reduce errors in interferometric heat transfer measurements caused by nanofluid nonuniformity.

Some studies have underscored the instability of nanofluids in problems involving conduction-dominated and convective flows [5, 7, 8]. To address this challenge, various techniques have been proposed to improve the stability of nanofluids. One such method involves using a probe sonicator. While there is consensus on its effectiveness in improving nanofluid stability, there is still no agreement on the optimal sonication time and power output [9, 10]. Another approach involves adding surfactants and controlling the pH of the mixture. Some studies have reported a reduction in stability [11] or negligible changes in stability [12] when surfactants like SDBS are added to Al<sub>2</sub>O<sub>3</sub>-water nanofluids. However, the majority of research indicates an improvement in nanofluid stability with the addition of surfactants [10]. Despite this, there is no consensus on the optimal surfactant concentration to be used [13-15]. Centrifugation is another method shown to improve the stability of nanofluids. Some studies [16, 17] attributed this enhanced stability to the reduction in the average size of nanoparticles. Sharma et al. [18] used a different approach by dividing the nanofluid container into five sections and analyzing the nanoparticle concentration in each to assess nanofluid stability.

This study utilizes a newly developed interferometric method to evaluate nanofluid stability. This technique visualizes and quantifies nanofluid concentration uniformity, providing a more detailed and reliable understanding of nanofluid stability compared to methods used in the literature. Using this approach, the research demonstrates interferometric heat transfer measurement errors when a temperature gradient is applied to a non-uniform nanofluid. To improve accurate heat transfer measurements in interferometric studies, the research investigates strategies for stabilizing the nanofluid, including ultrasonication, sedimentation, centrifugation, and SDBS addition.

## 2. Methodology

The experimental model, shown in Fig. 1. a-b, consists of a middle fluid chamber section between two optical windows with  $\lambda/10$  flatness, enclosed by Delrin end walls. The fluid chamber, divided by a 2.0 mm aluminum plate, contains two fluid cavities: the top cavity filled with deionized water (reference fluid) and the bottom with Al<sub>2</sub>O<sub>3</sub>-water nanofluid (test fluid). Each cavity has dimensions of 30.0 mm (length), 9.0 mm (width), and 10.0 mm (optical length), with a total volume of 2.7 ml. Temperature is monitored using three T-type thermocouples ( $\pm0.2$  °C accuracy), placed at the separating plate and the top and bottom aluminum plate surfaces. The experimental model is positioned between two heat exchangers and set up in a Mach-Zehnder interferometry (MZI) setup. For the stability measurement experiment, the two heat exchangers are maintained at room temperature (21.5°C), while temperature measurement experiments are conducted by setting the top and bottom heat exchangers to approximately 26.5°C and 16.5°C, respectively. More details about the experimental model can be found in our previous publications [2, 19].

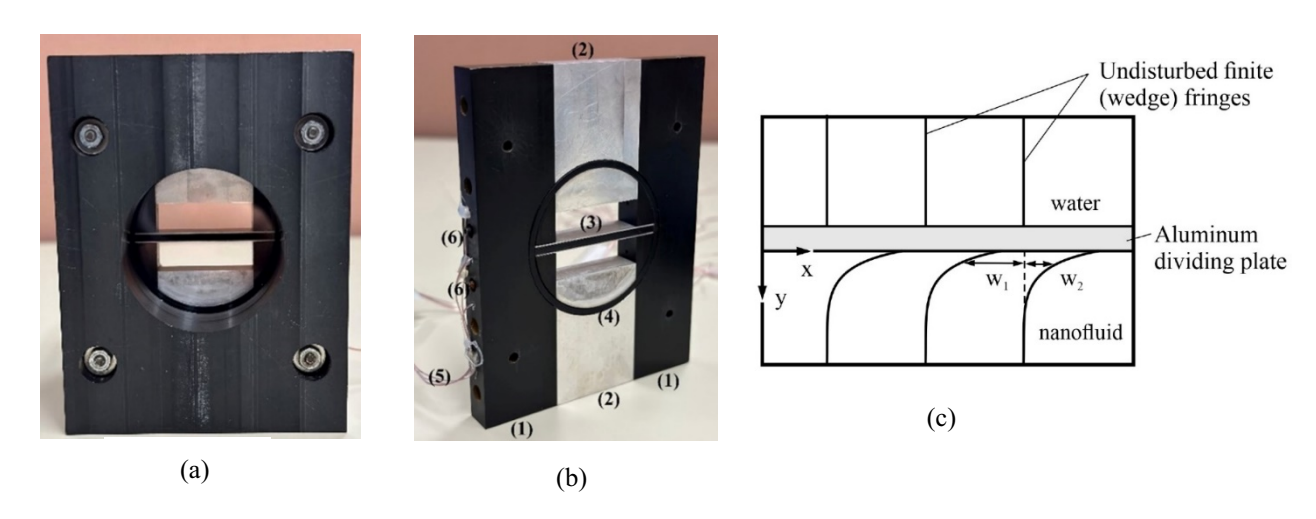


Fig.1: (a) Fully assembled model viewed along the beam direction, (b) Middle fluid chamber section depicting, (1) two Delrin side walls, (2) upper and lower aluminum plates, (3) middle-separating aluminum plate, (4) O-rings, (5) three thermocouples placed in their respective holes, and (6) the fluid injection holes, (c) Diagram of a finite fringe interferogram depicting the measurement of the concentration variations (Δφ) in an isothermal model.

The interferometer is set up to produce both infinite and finite fringes. In infinite fringe mode, the reference and test beams are aligned parallel upon recombination, resulting in uniform illumination without fringes under undisturbed conditions. On the other hand, in finite fringe mode, the reference beam recombines with the test beam at a small angle, creating a series of vertical interference fringes. Variations in refractive index due to changes in temperature  $(\Delta n_T)$  or concentration  $(\Delta n_{\phi})$  result in the emergence of fringes in the infinite mode and the bending of fringes in the finite mode. The total interference fringe shift  $(\Delta \varepsilon_{\text{tot}})$  observed in the output of the interferometer is the result of both the temperature-induced fringe shift  $(\Delta \varepsilon_{\text{T}})$  and the concentration-induced fringe shift  $(\Delta \varepsilon_{\phi})$ , and is represented as:

$$\Delta \varepsilon_{tot} = \Delta \varepsilon_T + \Delta \varepsilon_{\phi} = \frac{L}{\lambda_0} \Delta n_T + \frac{L}{\lambda_0} \Delta n_{\phi} = \frac{L \, dn}{\lambda_0 \, dT} \Delta T + \frac{L}{\lambda_0} \frac{dn}{d\phi} \Delta \phi \tag{1}$$

Where L and  $\lambda_0$  are the optical length of the model and the vacuum wavelength of the light source ( $\lambda_0$ =632.8 nm). Moreover, dn/dT and  $dn/d\phi$  represent the temperature and concentration coefficients of the refractive index, respectively, and can be found in the literature [20].

To assess the stability of the nanofluid, the finite fringe mode is set, and the model is maintained isothermally at room temperature to eliminate the first term in Eq. (1). In this case,  $\Delta \varepsilon$  can be obtained by  $w_2 / (w_1 + w_2)$ , as detailed in the literature [5], and therefore,  $\Delta \phi$  is expressed as:

$$\Delta \phi = \phi_0 - \phi = \frac{\lambda_0}{Ldn/d\phi} \left[ \frac{w_2}{w_1 + w_2} \right] \tag{2}$$

Where  $\phi_0$  and  $\phi$  represent far-field and target point concentrations. Moreover,  $w_1$  and  $w_2$  are horizontal distances measured on the interferogram, as illustrated in Fig. 1.c. To account for variations in initial nanofluid concentrations, the concentration difference is divided by the initial concentration using:

Normalized Instability Index (NII) [%] = 
$$\frac{|\Delta \phi|}{\phi_{(t=0)}} \times 100$$
 (3)

The normalized instability index (NII) uncertainty is estimated using the Kline and McClintock method [21] at 95% confidence. The results are  $\pm 6.2\%$  uncertainty in concentration difference [5] and  $\pm 3.1\%$  in  $\phi_{(t=0)}$ , resulting in an uncertainty of  $\pm 6.9\%$  in NII.

## 3. Nanofluid preparation and characterization

A known mass of  $Al_2O_3$  nanopowder (nominal diameter =13 nm,  $\rho = 4000 \ kg/m^3$ ) from Sigma Aldrich is dispersed in deionized water using a 600 W probe sonicator with a 5-second on/off alternating cycle to produce 250 mL of  $Al_2O_3$ -water nanofluid. Although the probe sonicator is the most effective mixing method [7], as will be shown, large particles remain in the suspension. Therefore, sedimentation and centrifugation are used to remove the larger particles.

In the sedimentation method, 150 mL of nanofluid is extracted from the middle of the container after leaving the sample undisturbed for 24 hours [2, 5, 6]. On the other hand, in the centrifugation method, the sample is placed into five 50 mL tubes and centrifuged at a relative centrifugal force (RCF) of 1500 g for 90 minutes. The top half of the nanofluid from each tube is then extracted and subjected to 30 minutes of ultrasonication with a 5-second on/off cycle to ensure uniformity. The final concentration of all samples is determined by drying a portion of each on a hot plate [5, 6]. To investigate the effect of the surfactant, the same concentration of SDBS (sodium dodecylbenzene sulfonate) as Al<sub>2</sub>O<sub>3</sub> is added to the nanofluid sample and subjected to an additional 30 minutes of ultrasonication. A summary of the nanofluid sample preparation procedures is represented in Table 1.

Table 1: Summary of preparation procedures and concentrations of the different nanofluid samples

Sample	Pre-processing concentration (wt. %)	Sedimentation time (hr)	RCF and Centrifugation time	Post- processing concentration (wt. %)	SDSB concent ration (wt. %)	Zeta potential (mV)	Mean particle diameter (nm)
1	0.16	-	-	0.16	0	35.8	1006.2
2	1.0	24	-	0.16	0	43.7	589.4
3	4.0	-	1500g, 90min	0.23	0	56.3	64.5
4	4.0	_	1500g, 90min	0.23	0.23	-55.7	60.9

The nanoparticle size distribution and zeta potential are measured using the Zetasizer Ultra instrument (Malvern Panalytical), as shown in Fig. 2 and Table 1. It can be seen that both sedimentation and centrifugation methods

effectively remove large particles and reduce the average nanoparticle size. Moreover, Sample 1 contains very large particles and is therefore not sufficiently transparent to be tested using the interferometric method.

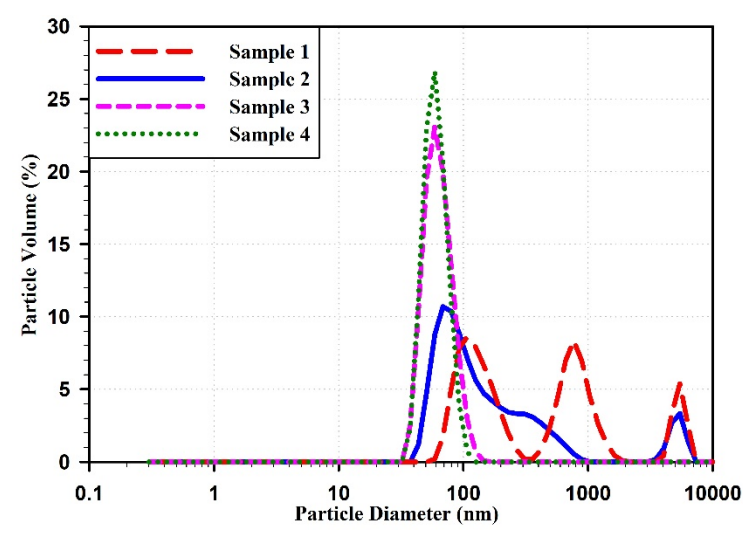


Fig. 2: DLS particle size distribution of nanoparticles in the Al<sub>2</sub>O<sub>3</sub>-water nanofluid.

#### 4. Results and discussion

In the first part of the study, Sample 2, prepared by the sedimentation method, is injected into the bottom cavity, while deionized water is injected into the top cavity of the experimental model, and observed for 3 hours under isothermal conditions. The infinite fringe interferograms at the initial time and after 3 hours are shown in Fig. 3 a-b. As depicted in Fig. 3.a, there is uniform illumination in the nanofluid cavity at the start, indicating that the nanofluid concentration is uniform. However, after 15 minutes, fringes begin to appear and propagate through the nanofluid cavity over 3 hours (Fig. 3.b) [5]. Since no temperature gradient is applied, these fringes are attributed to the non-uniformity of the nanofluid.

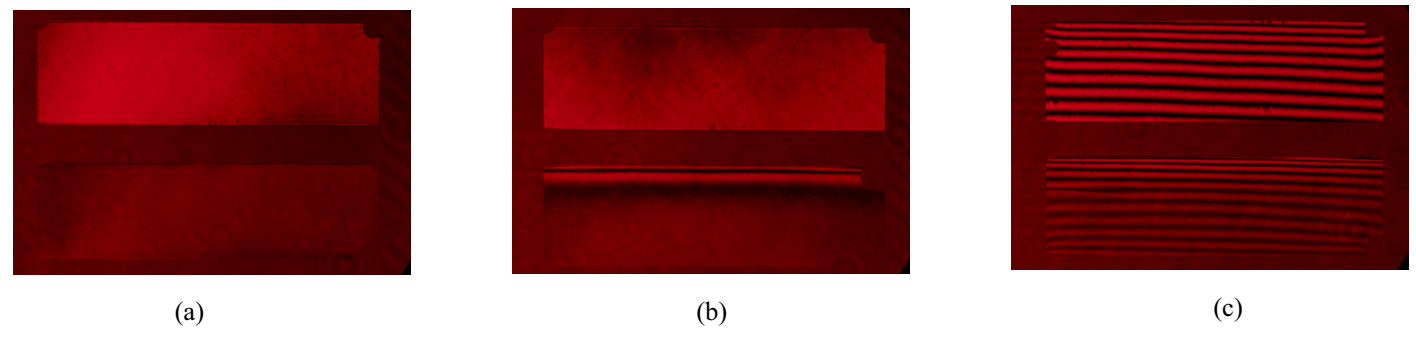


Fig. 3: Infinite interference fringe in deionized water (top cavity) and 0.16 wt.% Al<sub>2</sub>O<sub>3</sub>-water nanofluid prepared by the sedimentation method (bottom cavity): (a) under isothermal condition, initially (~30 seconds), (b) under isothermal condition after 3 hours, and (c) with a temperature difference of 10 °C after 3 hours.

In the next experiment, after injecting water and the same nanofluid (Sample 2), the experimental model is subjected to a 10°C temperature difference from top to bottom and observed for three hours. The interferogram captured after three hours under this temperature difference is shown in Fig. 3.c. With pure conduction occurring in both cavities and the low-concentration nanofluid used in the study having the same thermal conductivity as deionized water [2], the

fringes are expected to be evenly spaced in both cavities [2, 19]. However, while the fringes in the deionized water cavity are uniformly distributed, those in the upper region of the nanofluid cavity become closely spaced. This effect is caused by the superposition of concentration-induced fringes with temperature-induced fringes in the nanofluid upper region cavity. Assuming nanofluid stability can lead to misinterpreting the combined fringes as purely temperature-induced, resulting in significant errors in heat transfer measurements. Therefore, it is recommended that the interferograms be examined without a temperature gradient throughout the experiment to confirm nanofluid stability before conducting heat transfer experiments.

As can be seen, the sample prepared by the sedimentation method (Sample 2) is not stable enough for heat transfer experiments. Although large particles are partially removed in Sample 2 and it has a smaller average nanoparticle size (589.4 nm) compared to Sample 1 (1006.2 nm), which did not undergo sedimentation and centrifugation, the remaining large particles in Sample 2 still lead to instability (as shown in Fig. 2). These larger particles, with their higher settling rate, have been identified as the primary source of nanofluid instability [5]. To further improve the nanofluid stability, centrifugation is applied, and SDBS is added to the sample. Since finite fringes are more sensitive to concentration changes [5], the stability of the nanofluid samples is evaluated using finite fringe interferograms over 1.5 hours under isothermal conditions, as shown in Fig. 4.

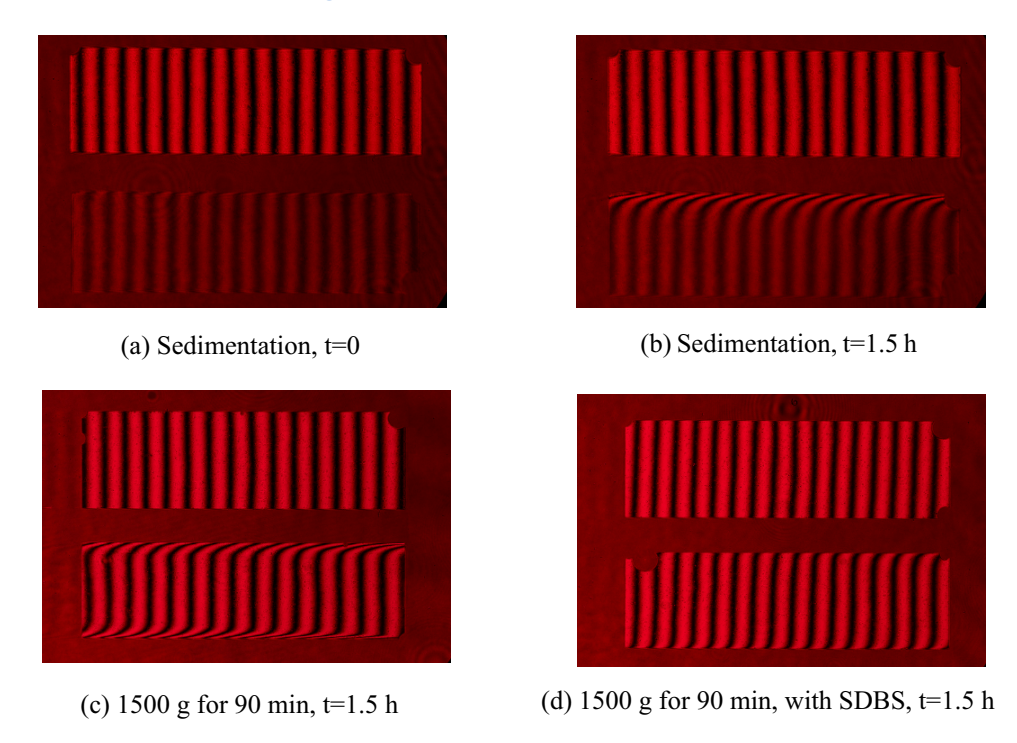


Fig. 4: Finite fringe interferograms of deionized water (top cavity) and Al<sub>2</sub>O<sub>3</sub>-water nanofluid (bottom cavity). (a) Initial state; (b–d) after 1.5 hours. Nanofluid preparation methods: (a, b) sedimentation (Sample 2), (c) Centrifugation at 1500 g for 90 min (Sample 3), (d) Centrifugation with 1500 g for 90 min with the addition of SDBS (Sample 4).

As shown in Fig. 4.a, the fringes are perpendicular to the aluminum surfaces in both the water and nanofluid cavities, indicating a uniform nanofluid at the initial time. Since all samples are initially uniform, the interferogram for each sample is perpendicular to the aluminum surface, and only one sample is shown for brevity (Fig. 4.a). Over time, however, the fringes begin to bend in Samples 2 and 3, indicating nanofluid instability. The instability at the top part of the nanofluid container is quantified using Eqs. 2 and 3 and is shown in Fig. 5.

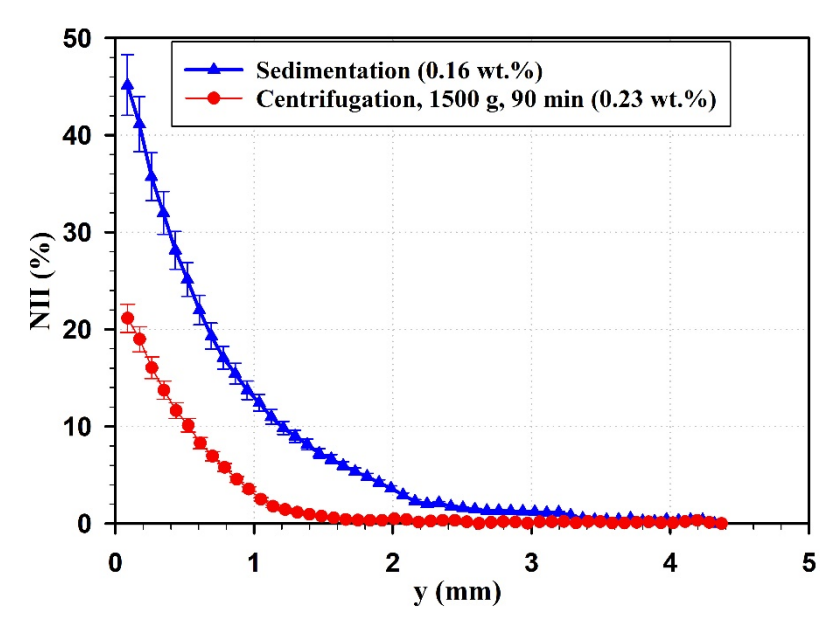


Fig. 5: Normalized instability index (NII) of Al<sub>2</sub>O<sub>3</sub>-water nanofluid produced by the sedimentation method and centrifugation at 1500 g for 90 minutes, where a lower NII indicates higher stability.

The results depicted in Fig. 5 demonstrate that centrifugation enhances nanofluid stability compared to the sedimentation method. This improvement corresponds to the lower mean particle diameter (64.5 nm) and higher zeta potential (56.3 mV) observed in the centrifuged sample (Sample 3) compared to the sedimented sample (Sample 2). Figure 4.d illustrates that the sample prepared using centrifugation at 1500 g for 90 minutes with the addition of SDBS (Sample 4) remains perpendicular to the aluminum surface after 1.5 hours, indicating its stability over this time. The NII value for this sample is 0 (indicating near-perfect stability) and, therefore, is not displayed in Fig. 5. This indicates that SDBS significantly improves the stability of the nanofluid.

Although the mean particle diameter and absolute zeta potential of Sample 4 are similar to those of Sample 3, Sample 4 exhibits higher stability. This enhanced stability can be attributed to the higher steric repulsion resulting from the addition of SDBS. SDBS stabilizes the nanofluid by adsorbing its hydrophobic segment onto the nanoparticle surface while extending its hydrophilic end into the water, thereby increasing the spacing between nanoparticles and reducing agglomeration [10]. This result highlights that while DLS and zeta potential are useful supplementary techniques for analyzing nanofluid stability, they cannot serve as standalone methods for assessing stability. Finally, in this study, an Al<sub>2</sub>O<sub>3</sub>-water nanofluid sample with a concentration of 0.23 wt.% was prepared using one hour of sonication followed by centrifugation at 1500 g for 90 minutes with 0.23 wt.% SDBS, resulting in a sample that remains stable for 1.5 hours. This duration is sufficient to conduct interferometric heat transfer experiments [2], which was the motivation for the current study.

#### 5. Conclusion

This study employs a newly developed interferometric method capable of visualizing and quantifying even minor nonuniformities in nanofluids to evaluate their stability. Additionally, DLS and zeta potential measurements were used as supplementary techniques to further analyze stability. The findings reveal that nonuniformities in nanofluids prepared using methods reported in the literature produce concentration-induced fringes, which are superimposed on temperature-induced fringes when a temperature difference is applied. This demonstrates that nanofluid instability has the potential to lead to significant errors in optical heat transfer measurements. To address these sources of error, different strategies were implemented to enhance nanofluid stability, including the removal of larger nanoparticles through sedimentation

and centrifugation, as well as the addition of SDBS. The results show that while sedimentation improves nanofluid stability, centrifugation is more effective. Additionally, the addition of SDBS further enhances stability. It was also shown that while DLS and zeta potential are effective, they cannot serve as sole indicators of stability. This study successfully produces a 0.23 wt.% Al<sub>2</sub>O<sub>3</sub>-water nanofluid with 0.23 wt.% SDBS that remains stable for 1.5 hours, making it suitable for interferometric heat transfer experiments.

## **Acknowledgments**

The support of the Natural Sciences and Engineering Research Council of Canada is gratefully acknowledged.

#### References

- [1] R.R. Souza, V. Faustino, I.M. Gonçalves, A.S. Moita, M. Bañobre-López, R. Lima, "Review of the Advances and Challenges in Measuring the Thermal Conductivity of Nanofluids," *Nanomaterials*, 2022, 12 (15), 2526.
- [2] S. Sahamifar, D. Naylor, T. Yousefi, J. Friedman, "Measurement of the thermal conductivity of nanofluids using a comparative interferometric method," *International Journal of Thermal Sciences*, 2024, 199, 108890.
- [3] S.S. Rao, A. Srivastava, "Whole field measurements to understand the effect of nano-particle concentration on heat transfer rates in a differentially-heated fluid layer," *Exp Therm Fluid Sci*, 2018, 92:326–45.
- [4] S.S. Rao, A. Srivastava, "Measuring thermal diffusivity of dilute nanofluids using interferometry-based inverse heat transfer approach," *J. Thermophys. Heat Tran.*, 2020, 34 (3) 476–487.
- [5] S. Sahamifar, D. Naylor, J. Friedman, "An interferometric method to visualize and quantify nanofluid stability," *International Journal of Heat and Mass Transfer*, 2024, Volume 235, 126197.
- [6] S. Sahamifar, D. Naylor, J. Friedman, "Effect of Non-Uniform Nanofluid Concentration on Interferometric Heat Transfer Measurements," *International Journal of Thermal Sciences*, 2024, under review. Pre-print available at SSRN https://ssrn.com/abstract=4938693 or http://dx.doi.org/10.2139/ssrn.4938693.
- [7] J. Hong, S. Liu, Y. Yan, P. Glover, "Experimental measurement of dynamic concentration of nanofluid in laminar flow," *Exp. Therm. Fluid Sci.*, 2017, 88, 483-489.
- [8] E. Khalili, A. Saboonchi, M. Saghafian, "Experimental study of nanoparticles distribution on natural convection of Al2O3-water nanofluid in a square cavity," *Int. J. Therm. Sci.*, 2017, 112, 82–91.
- [9] A.R.I. Ali, B. Salam, "A review on nanofluid: Preparation, stability, thermophysical properties, heat transfer characteristics and application," *SN Appl. Sci.*, 2020, 2, 1636.
- [10] L. Kong, J. Sun, Y. Bao, "Preparation, characterization and tribological mechanism of nanofluids," *Rsc Adv.* 7, 2017 12599–12609.
- [11] J. Ji, X. Yao, J. Gao, W. Lu, W. Wang, D. Chu, "Effect of surfactants and pH values on stability of γ-Al2O3 nanofluids," *Chem. Phys. Lett.*, 2021 Oct, 16 (781) 138996.
- [12] B. Mehta, D. Subhedar, "Synthesis and characterization of γ-Al2O3-Water nanofluid with and without surfactant," *Mater. Today: Proc.* 62 (2022), 418-425.
- [13] A. Gallego, K. Cacua, B. Herrera, D. Cabaleiro, M.M. Pi<sup>\*</sup>neiro, L. Lugo, "Experimental evaluation of the effect in the stability and thermophysical properties of water- Al2O3 based nanofluids using SDBS as dispersant agent," *Adv Powder Technol*, 2019.
- [14] M.F. Zawrah, R.M. Khattab, L.G. Girgis, H. El Daidamony, R.E. Abdel Aziz, "Stability and electrical conductivity of water-base Al2O3 nanofluids for different applications," *HBRC Journal*, 2016, 12 (3), 227–234.
- [15] D. Zhu, X. Li, N. Wang, X. Wang, J. Gao, H. Li, "Dispersion behavior and thermal conductivity characteristics of Al2O3–H2O nanofluids," *Curr. Appl. Phys.*, 9 (2009) 131–139.
- [16] J. Lee, Y.-J. Yoon, J.K. Eaton, K.E. Goodson, S.J. Bai, "Analysis of Oxide (Al2O3, CuO, and ZnO) and CNT Nanoparticles Disaggregation Effect on the Thermal Conductivity and the Viscosity of Nanofluids," *Int. J. Precis. Eng. Manuf.*, 15 (2014) 703–710.
- [17] B. Du, Q. Jian, "Size controllable synthesis of graphene water nanofluid with enhanced stability," *Fullerenes Nanotub Carbon Nanostruct.*, 2019;27(1):87–96.

- [18] B. Sharma, S.K. Sharma, S.M. Gupta, A. Kumar, "Modified two-step method to prepare long-term stable CNT nanofluids for heat transfer applications," *Arab. J. Sci. Eng.*, 43 (2018) 6155–6163.
- [19] S. Sahamifar, D. Naylor, T. Yousefi, J. Friedman, "Designing a Comparative Interferometric Method for Measuring the Thermal Conductivity of Transparent Fluids," Proceedings of the 11th International Conference on Fluid Flow, Heat and Mass Transfer (FFHMT 2024), No. 033.
- [20] T. Yousefi, D. Naylor, M.Z. Saghir, "Refractive index and temperature coefficient of refractive index of Al2O3-and SiO2-water nanofluids," *International Journal of Thermofluids*, 2022, 16, 100238.
- [21] S.J. Kline, F.A. McClintock, "Describing uncertainties in single sample experiments," Mechanical Engineering, 75 (1953), pp. 3-8.